**Supplementary Information**

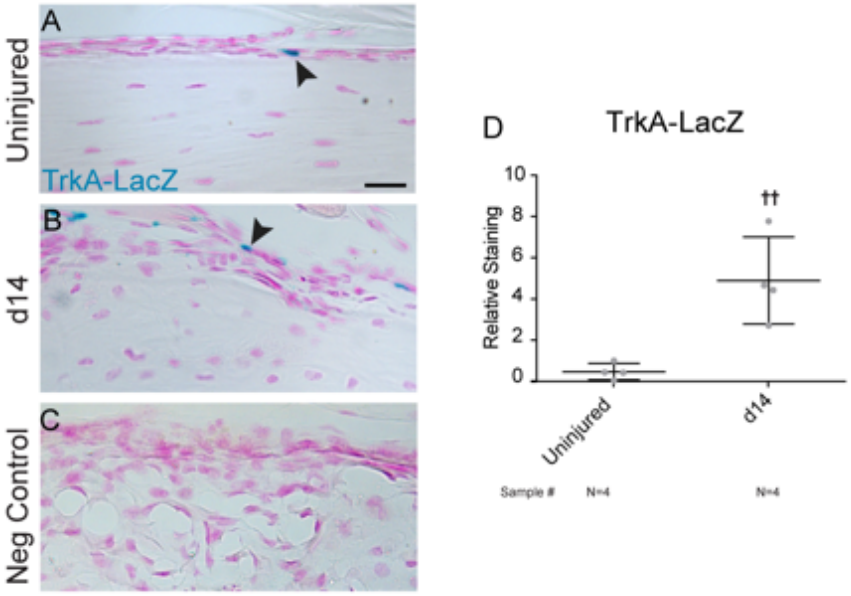


**Supplementary Figure S1. TrkA reporter activity after stress fracture. (A,B)** High magnification images of Xgal stained sections among TrkA-LacZ reporter animals, including **(A)** uninjured control and **(B)** callus at d14 post-injury. **(C)** Negative control confirming absence of staining in a $LacZ^-$ fracture callus. **(D)** Quantification of TrkA-LacZ reporter activity, comparing d14 post-fracture to uninjured control. In graphs, each dot represents a single sample, with sample number stated below. Black scale bar: 20 μm. †† $P<0.01$ in comparison to uninjured control as determined using a two-way Student's *t*-test.

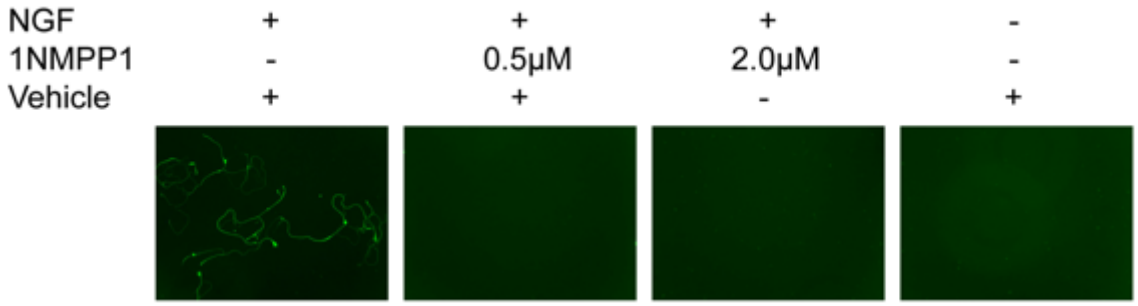


**Supplementary Figure S2. Validation of 1NMPP1 inhibition of NGF mediated DRG derived dendrite growth *in vitro*.** Dissociated DRG neuron cultures were established from TrkA$^{F592A}$ animals (e13.5) and cultured for 96 h with 1NMPP1 (0.5 or 2 μM) or vehicle control (DMSO with PBST (0.25% Tween20 in PBS)) with or without recombinant Nerve growth factor (NGF, 50 ng/mL). Immunofluorescent staining for neurofilament demonstrates dendrite growth with NGF, which is completely inhibited by the presence of 1NMPP1. Experiment was performed in a single replicate.

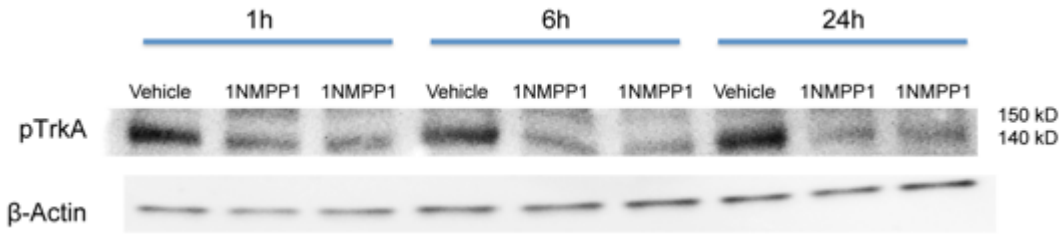


**Supplementary Figure S3. Validation of 1NMPP1 inhibition of TrkA phosphorylation within the dorsal root ganglia (DRG) *in vivo*.** The small molecule 1NMPP1 (17 μg/g BW IP) or vehicle control (50% DMSO and 50% PBST (0.25% Tween20 in PBS)), was administered to $TrkA^{F592A}$;Thy1-YFP animals (male, 15 week old). Bilateral DRG were pooled (L2-L5) from each animal and protein was immediately isolated for analysis of phospho-TrkA by Western blot. Each lane represents pooled lumbar DRGs from a single animal. Experiment was performed in two replicates.

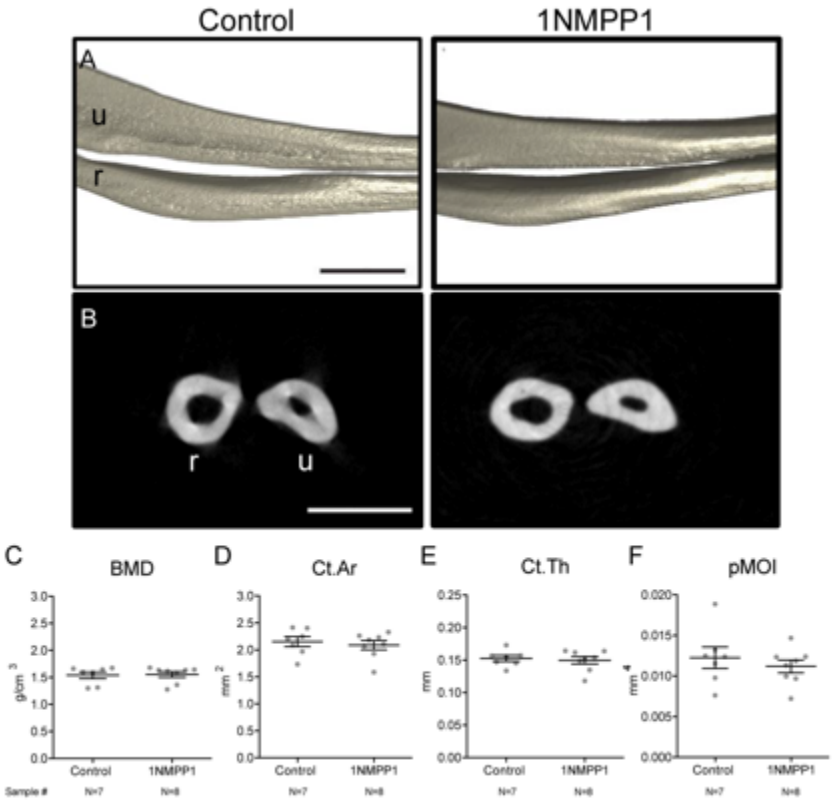


**Supplementary Figure S4. Lack of cortical bone phenotype in uninjured forelimbs of 1NMPP1-treated TrkA 592A animals.** Analysis of uninjured forelimbs among $TrkA^{F592A}$;Thy1-YFP mice treated with 1NMPP1 or vehicle control for 7 d. **(A,B)** μCT images of mid-diaphysis of uninjured forelimb of $TrkA^{F592A}$;Thy1-YFP mice treated with 1NMPP1 or vehicle control, including **(A)** three dimensional μCT reconstruction and **(B)** axial cross-sectional images. **(C-F)** Quantitative μCT analysis of the ulnar mid-diaphysis among $TrkA^{F592A}$;Thy1-YFP mice treated with 1NMPP1 or vehicle control, including **(C)** Bone Mineral Density (BMD), **(D)** Cortical Area (Ct.Ar), **(E)** Cortical Thickness (Ct.Th), and **(F)** polar Moment of Inertia (pMOI). For all graphs, each dot represents a single sample, with each sample number stated below. Black scale bar: 500 μm; white scale bar: 1mm. u: ulna; r: radius. No statistically significant differences as determined using a two-way Student's *t*-test.

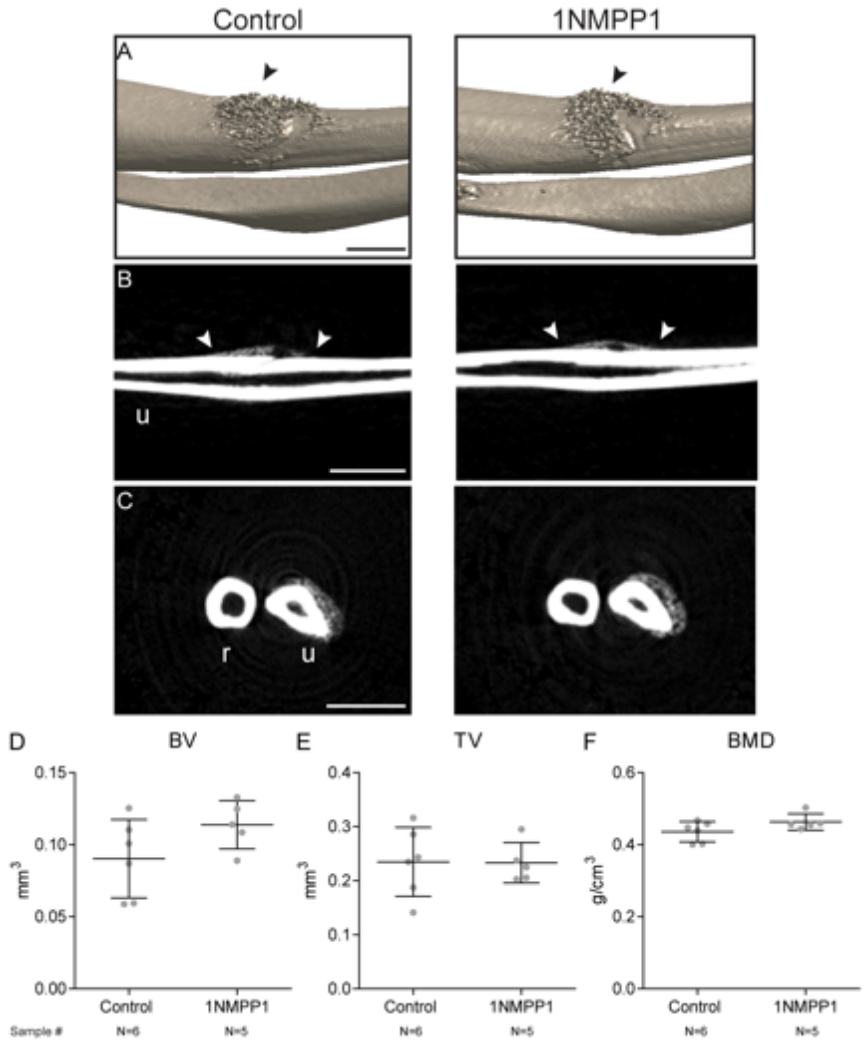


**Supplementary Figure S5. Lack of stress fracture phenotype in 1NMPP1-treated wildtype animals. (A-C)** μCT images of ulnar stress fracture healing among C57BL/6J mice treated with 1NMPP1 or vehicle control at d7 post-injury. **(A)** μCT reconstructions, **(B)** coronal cross sectional images, and **(C)** axial cross sectional images are shown. u: ulna; r: radius. **(D-F)** Quantitative μCT analysis of the ulnar stress fracture after 7d among C57BL/6J mice treated with 1NMPP1 or vehicle control, including **(D)** Bone Volume (BV), **(E)** Tissue Volume (TV), and **(F)** Bone Mineral Density (BMD). For all graphs, each dot represents a single sample, with each sample number stated below. Black scale bar: 500 μm; white scale bar: 1mm. u: ulna; r: radius. No statistically significant differences as determined using a two-way Student's *t*-test.

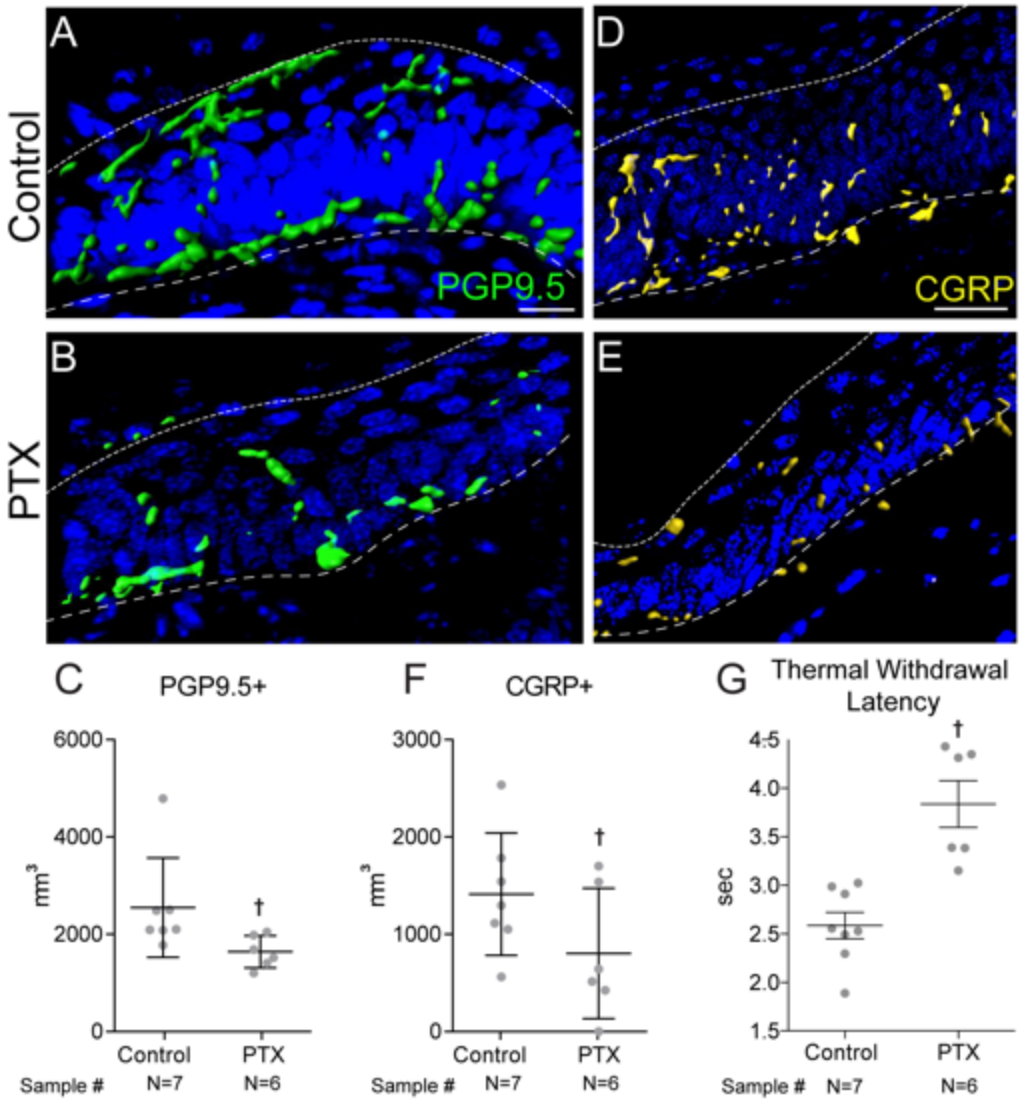


**Supplementary Figure S6. Paclitaxel (PTX) induces a peripheral sensory neuropathy. (A-C)** Intra-epidermal nerve fiber loss among PTX-treated animals in comparison to control, including **(A,B)** representative pan-neuronal PGP9.5 immunohistochemical staining, appearing green, and **(C)** quantification of $PGP9.5^{+}$ nerve fiber frequency. **(D-F)** Peptidergic intra-epidermal nerve fiber loss among PTX-treated animals, including **(D,E)** representative Calcitonin gene-related peptide (CGRP) immunohistochemical staining, appearing yellow, and **(F)** quantification of $CGRP^{+}$ nerve fiber frequency. **(G)** Thermal withdrawal latency among control- or PTX-treated animals. Immunofluorescent images are presented as Imaris surface renderings. For all graphs, each dot represents a single sample, with sample numbers stated below. † $P<0.05$ in comparison to control as determined using a two-way Student's *t*-test. White scale bar: 20 μm.

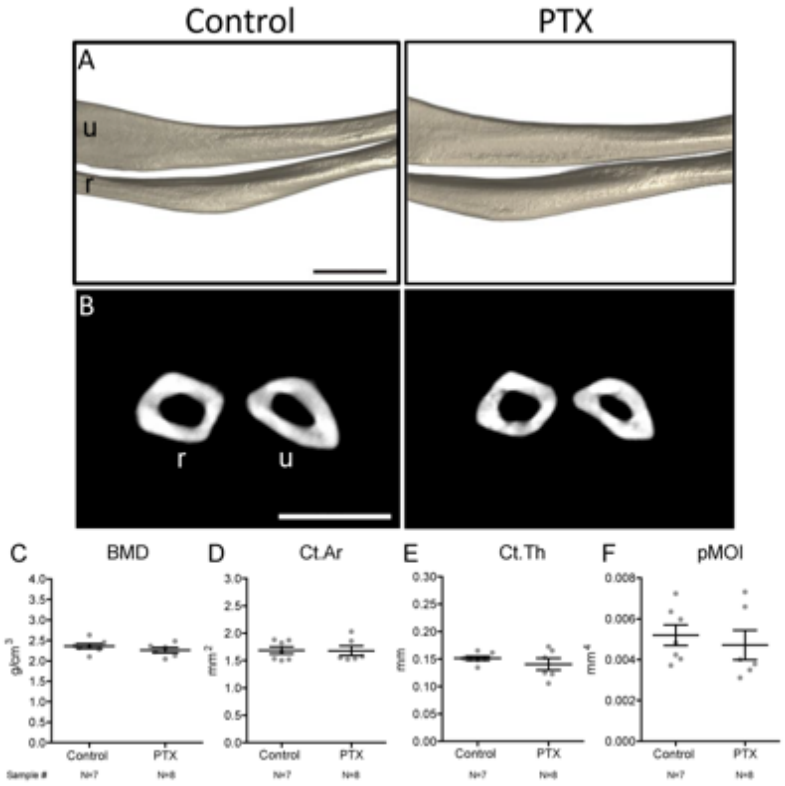


**Supplementary Figure S7. Lack of cortical bone phenotype in uninjured forelimbs of mice with Paclitaxel (PTX)-induced sensory neuropathy.** Analysis of uninjured forelimbs of PTX- or control-treated mice. Analysis performed at the study endpoint using uninjured, contralateral limbs. **(A,B)** μCT images of mid-diaphysis of uninjured forelimb, including **(A)** three dimensional reconstruction and **(B)** axial cross-sectional images. **(C-F)** Quantitative μCT analysis of the ulnar mid-diaphysis among PTX- and control-treated mice, including **(C)** Bone Mineral Density (BMD), **(D)** Cortical Area (Ct.Ar), **(E)** Cortical Thickness (Ct.Th), and **(F)** polar Moment of Inertia (pMOI). For all graphs, each dot represents a single sample, with each sample number stated below. Black scale bar: 500 μm; white scale bar: 1mm. u: ulna; r: radius. No statistically significant differences as determined using a two-way Student's *t*-test.

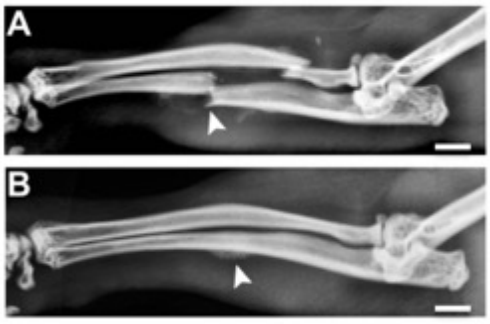


**Supplementary Figure S8. Method of screening for displaced fractures**. High resolution roentgenography (XR, Faxitron Bioptics, LLC, Tucson, AZ) assessed for either a displaced ulnar fracture and/or combined radial/ulnar fracture which occurred in a small minority of cases. These were discarded without analysis. **(A)** Displaced and combined radial/ulnar fracture (day 7 post injury shown). **(B)** For comparison, normal XR appearance of ulnar stress fracture at day 7 post injury, with intact bone and a localized callus most prominent on the ulnar aspect of the mid-diaphysis.

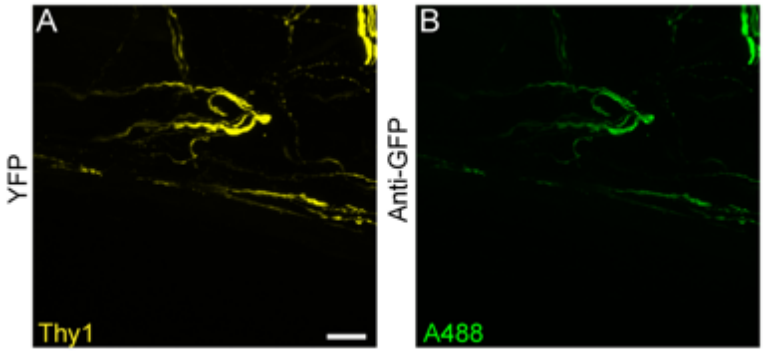


**Supplementary Figure S9. Validation of Thy1-YFP reporter activity without antibody detection.** No antibody detection was required to visualize fine nerve fibers using the Thy1-YFP reporter animal. Incubation was performed with anti-GFP antibody on Thy1-YFP reporter sections (day 14 fracture callus), followed by confocal microscopy and spectral unmixing to detect endogenous YFP reporter activity **(A)** or the exogenous fluorophore (Alexa Fluor 488) **(B)**. No difference in nerve frequency or distribution was seen. Representative images are shown, representing triplicate experimental replicates. White scale bar: 50 μm.

**Supplementary Table S1. Mouse lines used.**

| | |
|---|---|
| C57BL/6J | Jackson Laboratory, Stock #000664 |
| NGF-eGFP | Donated from Kawaja laboratory |
| Thy1-YFP | Jackson Laboratory, Stock #003709 |
| TrkA-LacZ | Jackson Laboratory, Stock #004837 |
| $TrkA^{F592A}$ | Donated from Ginty laboratory, Jackson Laboratory, Stock #022362 |

**Supplementary Table S2: Loading parameters by strain**

| **Genotype** | **Gender** (M/F) | **Age** (wks) | **Ultimate Force** (±SD) (N) | **Displacement Constant** (±SD) (mm) |
|---|---|---|---|---|
| C57BL/6J | M | 18 | -4.598 (±0.231) | -0.909 (±0.249) |
| NGF-eGFP | M | 18 | -4.616 (±0.325) | -0.945 (±0.333) |
| Thy1-YFP | M | 18 | -4.392 (±0.811) | -0.820 (±0.149) |
| TrkA-LacZ | M | 18 | -4.374 (±0.526) | -0.867 (±0.102) |
| $TrkA^{F592A}$;Thy1-YFP | M | 18 | -4.392 (±0.391) | -0.738 (±0.053) |

**Supplementary Table S3: Antibodies used.**

| Name | Vendor | Catalog No. | Concentration | |
|---|---|---|---|---|
| Anti-β-actin | Cell Signaling | 3700S | 1:2000 | WB |
| Anti-CD31 | Abcam | ab28364 | 1:100 | IF |
| Anti-CD45 | BioLegend | 103144 | 1:200 | IF |
| Anti-CD68 | Abcam | ab955 | 1:200 | IF |
| Anti-CD117 | LSBio | C177669 | 1:200 | IF |
| Anti-CGRP | Sigma Aldrich | C8198 | 1:200 | IF |
| Anti-F4/80 | Abcam | ab204467 | 1:200 | IF |
| Anti-GFP | Invitrogen | A21311 | 1:200 | IF |
| Anti-Ly-6G | BioLegend | 127636 | 1:200 | IF |
| Anti-Neurofilament | ThermoFisher | MA1-10041 | 1:1000 | IF |
| Anti-Osteocalcin | Abcam | ab93876 | 1:200 | IF |
| Anti-PDGFRα | Abcam | ab15501 | 1:200 | IF |
| Anti-PDGFRß | Abcam | ab32570 | 1:200 | IF |
| Anti-PGP 9.5 | Biorad | 7863-0504 | 1:200 | IF |
| Anti-TH | EMD Millipore | AB152 | 1:200 | IF |
| Anti-TRAP | Abcam | ab212723 | 1:500 | IF |
| Anti-pTrkA | Cell Signaling | 4619 | 1:1000 | WB |
| Anti-TUBB3 | Abcam | ab18207 | 1:1500 | IF |
| Anti-Vimentin | Abcam | ab194719 | 1:200 | IF |
| Goat Anti-Mouse IgG | Abcam | ab150119 | 1:200 | IF |
| Goat Anti-Rabbit IgG | Vector | DI-1594 | 1:200 | IF |